Isometric Embeddings in Binary Black Hole Merger Simulations

Iago Mendes, Hengrui Zhu, Robert Owen

April 3, 2024

Table of contents

Isometric Embeddings

The Isometric Embedding Problem

- Consists in visualizing a surface in 3D Euclidean space that would have the same metric as a given geometry.
- Embedding equations:

$$ds^2 = g_{\theta\theta}\, d\theta^2 + g_{\phi\phi}\, d\phi^2 + 2g_{\theta\phi}\, d\theta d\phi \tag{1}$$

$$ds^2 = dx^2 + dy^2 + dz^2 \tag{2}$$

$$\Rightarrow \begin{cases} (\partial_\theta x)^2 + (\partial_\theta y)^2 + (\partial_\theta z)^2 = g_{\theta\theta} \\ (\partial_\theta x)(\partial_\phi x) + (\partial_\theta y)(\partial_\phi y) + (\partial_\theta z)(\partial_\phi z) = g_{\theta\phi} \\ (\partial_\phi x)^2 + (\partial_\phi y)^2 + (\partial_\phi z)^2 = g_{\phi\phi} \end{cases} \tag{3}$$

- Known to be difficult to solve in general since the foundations of differential geometry. Being quadratic in the highest-order derivatives, equation (3) cannot be solved with usual PDE algorithms.

Motivations

- Remove arbitrariness when visualizing apparent horizons.
    - Current visualizations depend on the choice of coordinates.
- Useful for computing quasilocal quantities such as mass, energy, and angular momentum.

Remarks

- Not all 2-geometries are embeddable.
  - Famous example: Kerr black hole with dimensionless spin $\chi = a/M > \sqrt{3}/2$.
- Embeddings are unique only up to translational and rotational degrees of freedom in Euclidean space.

Numerical Methods

Matrix Method

- Adapted from Tichy et al.[1]
- Pseudospectral collocation: represent the embedding functions $x^i \in \{x, y, z\}$ as an expansion of basis functions.

$$x^i(\theta,\phi) = d^{in} D_n(\theta,\phi) \tag{4}$$

$$\Rightarrow \partial_A x^i(\theta,\phi) = d^{in}\, \partial_A D_n(\theta,\phi) \tag{5}$$

$$D_n(\theta,\phi) \longleftrightarrow Y_{\ell,m}(\theta,\phi)$$

- Solve for the coefficients d^{in} using Newton-Raphson iterations. At each step, we find δd^{in} using LAPACK's `dgelsy` routine.[2]

[1] Wolfgang Tichy *et al* 2015 Class. Quantum Grav. **32** 015002

[2] This least-squares matrix solver scales poorly with resolution.

Relaxation Method

- Idea: find the dyad vectors $\vec{e}_A \in \{\vec{e}_\theta, \vec{e}_\phi\}$, which are the basis vectors of $A \in \{\theta, \phi\}$.
$$\partial_A \vec{x} = \vec{e}_A \tag{6}$$
- To be a valid coordinate basis, $\vec{e}_\theta$ and $\vec{e}_\phi$ need to commute.
$$[\vec{e}_\theta, \vec{e}_\phi] := \partial_\theta \vec{e}_\phi - \partial_\phi \vec{e}_\theta \to 0 \tag{7}$$
- With (6), the embedding equations become
$$\vec{e}_A \cdot \vec{e}_B = g_{AB}. \tag{8}$$
- Approach: rotate $\vec{e}_A$ to achieve (7) and damp any violations of the constraints (8).
- Once we have $\vec{e}_A$, we solve (6) for $\vec{x}$.

Relaxation Method

g_{AB}

Dyad Rotation & Constraint Damping

$$\dot{\vec{e}}_A = \vec{\omega} \times \vec{e}_A - \gamma m^{CD} \mathcal{C}_{AC} \vec{e}_D$$

$$\vec{\omega} := \vec{e}_\phi \times D_\theta[\vec{e}_\theta, \vec{e}_\phi] - \vec{e}_\theta \times D_\phi[\vec{e}_\theta, \vec{e}_\phi]$$

$$\mathcal{C}_{AB} := \vec{e}_A \cdot \vec{e}_B - g_{AB}$$

$\vec{e}_\theta, \vec{e}_\phi$

Surface Construction

$$\nabla^2 \vec{x} = \frac{1}{\sin\theta} \partial_\theta (\sin\theta \, \vec{e}_\theta) + \frac{1}{\sin^2\theta} \partial_\phi (\vec{e}_\phi)$$

$\vec{x}$

Figure 1: Summary of the relaxation method.

Code Implementations

- Both methods were implemented on the Spectral Einstein Code (`SpEC`), which was used for all results presented here.
- As the relaxation method is a novel algorithm, we initially wanted to test it separately. Then, we created the Finite Difference Embedding Code (`FiDEC`), which is open-source.[3]

[3] Link to `FiDEC` is at the end of the presentation.

Test Cases

Selected Test Surfaces

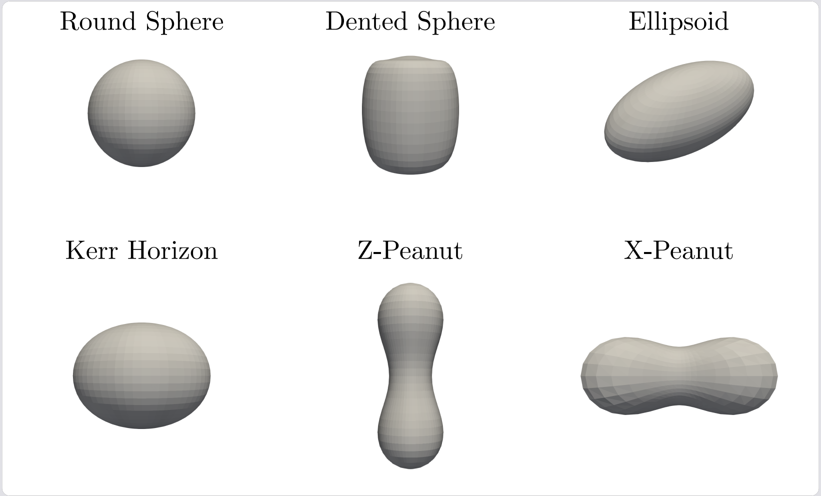

Figure 2: Selected surfaces used as test cases for the relaxation and matrix methods.

Convergence

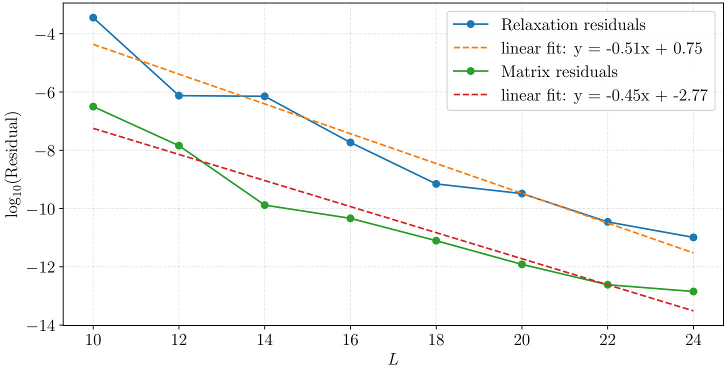

Figure 3: Convergence plot[4] for a Kerr horizon with $\chi = 0.7$.

[4] We define our residuals as $R_{AB} := (\partial_A \vec{x}) \cdot (\partial_B \vec{x}) - g_{AB}$, from which we get a norm and average over the surface to get a scalar.

Time Scaling

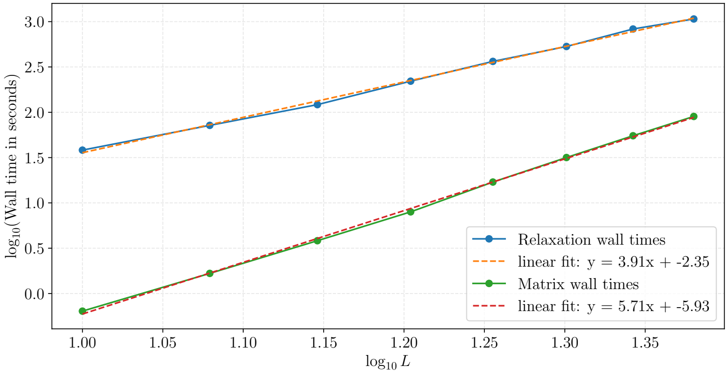

Figure 4: Time scaling plot for a Kerr horizon with $\chi = 0.7$. The relaxation method scales as $\sim O(L^4)$, whereas the matrix method scales as $\sim O(L^6)$.

Kerr Embeddability Limit

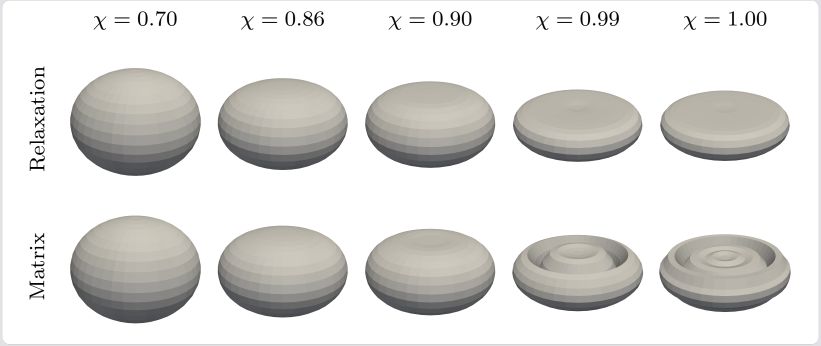

Figure 5: Comparison between embedding results from the relaxation and matrix methods as we approach and exceed the embeddability limit $\sqrt{3}/2 \approx 0.866$.

Kerr Embeddability Limit (continued)

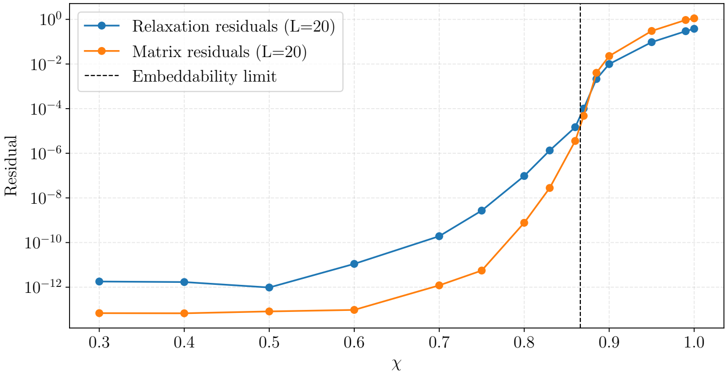

Figure 6: Residuals of the relaxation and matrix methods as we vary the dimensionless spin χ past the embeddability limit $\sqrt{3}/2 \approx 0.866$ for a resolution of $L = 20$.

Kerr Embeddability Limit (continued)

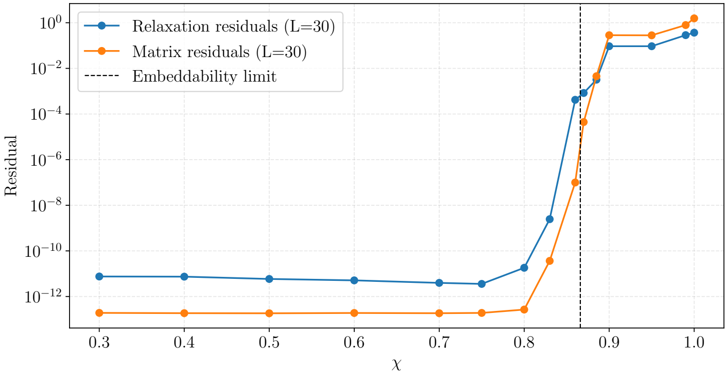

Figure 7: Residuals of the relaxation and matrix methods as we vary the dimensionless spin χ past the embeddability limit $\sqrt{3}/2 \approx 0.866$ for a resolution of $L = 30$.

BBH Merger Simulations

Equal-mass Non-spinning $q = 1;\ \chi_A = \chi_B = (0, 0, 0)$

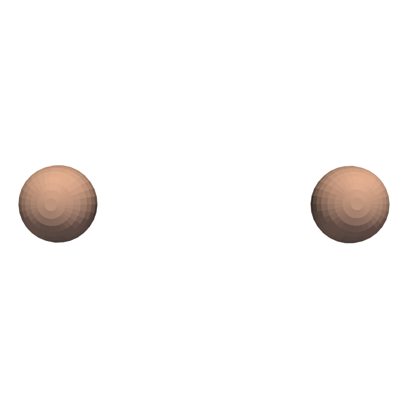

Video 1: Evolution of isometric embeddings.

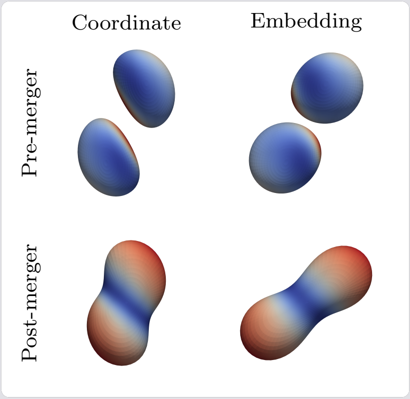

Figure 8: Coordinate shapes vs. isometric embeddings.

Co-aligned $q = 1;\ \chi_A = \chi_B = (0, 0, 0.6)$

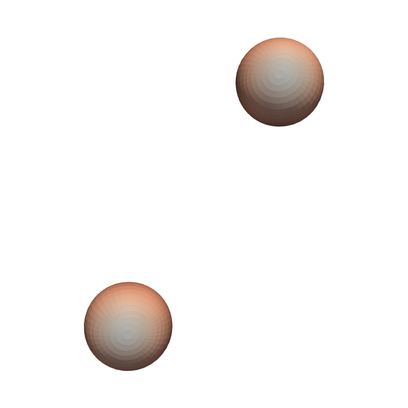

Video 2: Evolution of isometric embeddings.

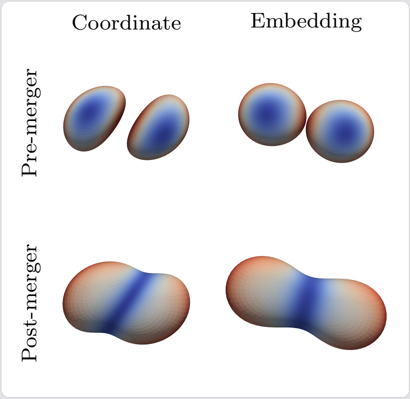

Figure 9: Coordinate shapes vs. isometric embeddings.

Anti-aligned

$q = 4;\ \chi_A = \chi_B = (0, 0, -0.6)$

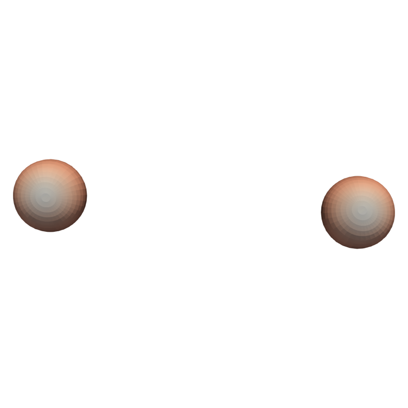

Video 3: Evolution of isometric embeddings.

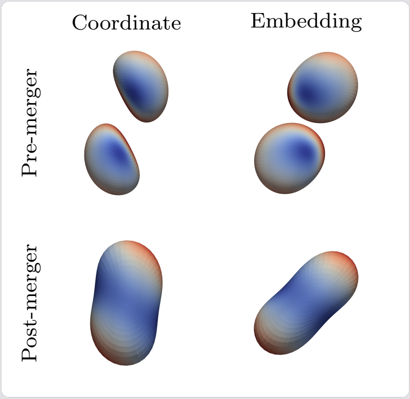

Figure 10: Coordinate shapes vs. isometric embeddings.

Nontrivial Mass Ratio

$q = 4; \ \chi_A = \chi_B = (0, 0, 0)$

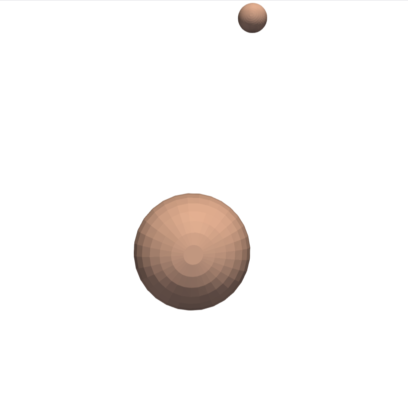

Video 4: Evolution of isometric embeddings.

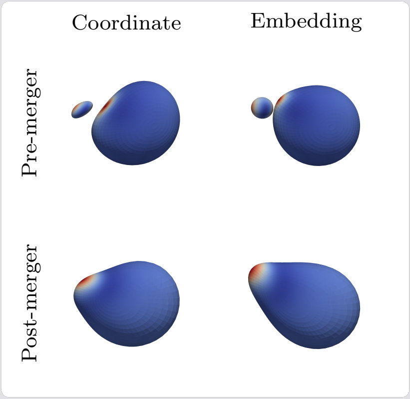

Figure 11: Coordinate shapes vs. isometric embeddings.

Generic $q = 2;\ \chi_A = (0.3, -0.4, 0.2);\ \chi_B = (0.2, 0.1, -0.3)$

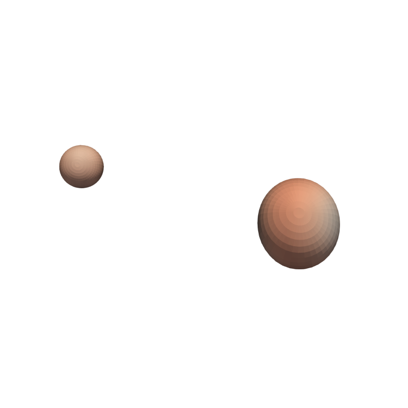

Video 5: Evolution of isometric embeddings.

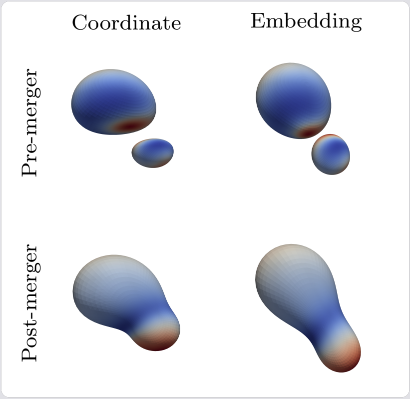

Figure 12: Coordinate shapes vs. isometric embeddings.

Non-embeddability?

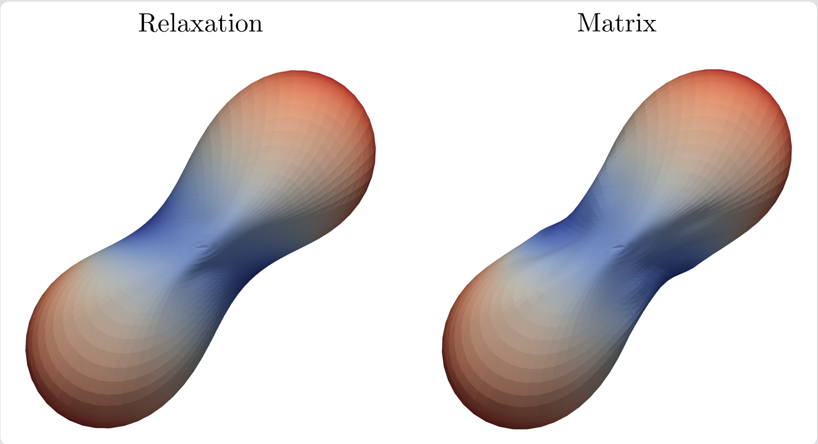

Figure 13: Failed embedding results from the relaxation method versus the matrix method for the anti-aligned run.

Non-embeddability? (continued)

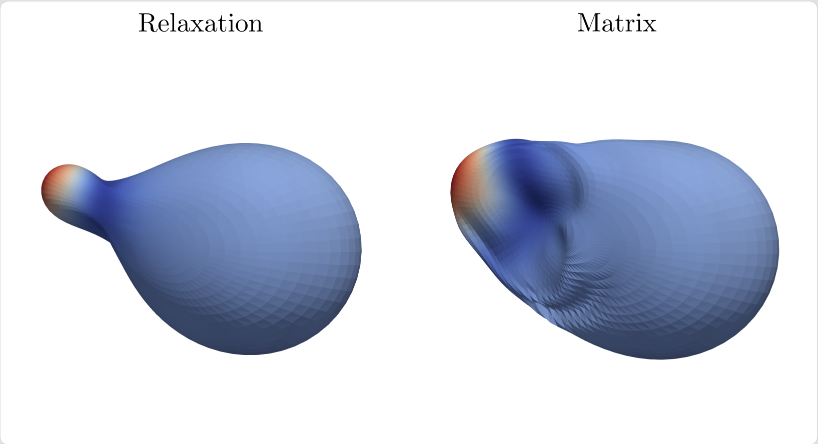

Figure 14: Failed embedding results from the relaxation method versus the matrix method for the $q = 4$ run.

Conclusion

Summary

- We have developed two efficient numerical methods for the isometric embedding problem in `SpEC`.
- Through test cases, we confirmed that they converge and analyzed their behavior.
- We applied these methods to numerical horizons in BBH merger simulations.

Future Work

- **Critical embedding**: understand how numerical horizons become embeddable or non-embeddable.
- **Wang-Yau quasilocal mass**: generalize our methods to Minkowski space.[5]
- **Gauge conditions**: use embedding results to choose gauge conditions that lead to more round apparent horizons (and faster mergers).

[5] Mu-Tao Wang and Shing-Tung Yau. "Quasilocal mass in general relativity". *Phys. Rev. Lett.*, 102:021101, Jan 2009.

Thank you! Any Questions?

More Details

iagomendes.com/embedding

Extra Slides

Wall Times

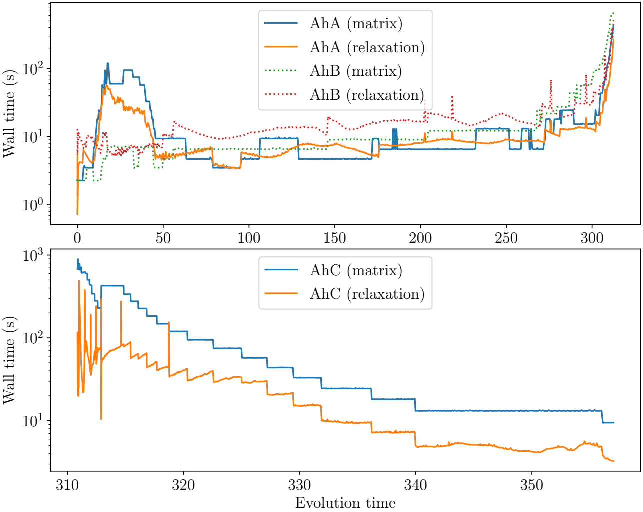

Figure 15: Generic run.

Wall Times (continued)

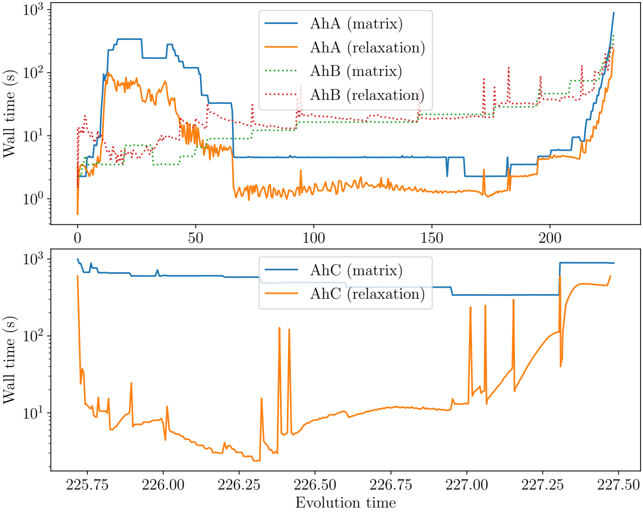

Figure 16: $q = 4$ run.

Residual Evolution

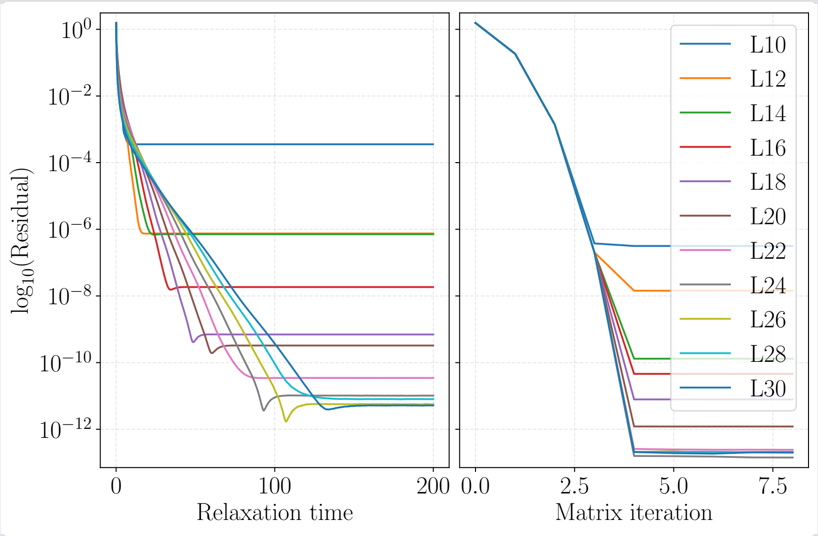

Figure 17: Kerr Horizon.

Relaxation Residual Distribution

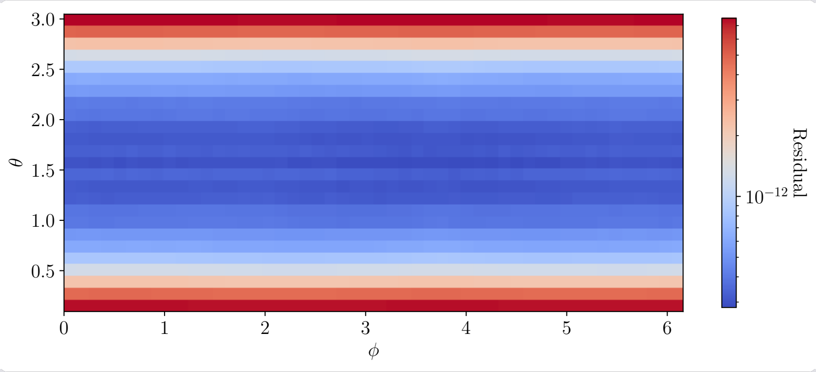

Figure 18: Kerr Horizon.